Available online at www.sciencedirect.com

ScienceDirect

Mendeleev Commun., 2023, **33**, 812–814

Mendeleev Communications

Single-atom alloy Pd_1Ag_{10}/Al_2O_3 catalyst: effect of CO-induced Pd surface segregation on the structure and catalytic performance in the hydrogenation of C_2H_2

Pavel V. Markov,[a] Nadezhda S. Smirnova,[a] Galina N. Baeva,[a] Igor S. Mashkovsky,[a] Andrey V. Bukhtiyarov,[b] Igor A. Chetyrin,[b] Yan V. Zubavichus[b] and Alexander Yu. Stakheev*[a]

[a] *N. D. Zelinsky Institute of Organic Chemistry, Russian Academy of Sciences, 119991 Moscow, Russian Federation. Fax: +7 499 135 5328; e-mail: st@ioc.ac.ru*

[b] *G. K. Boreskov Institute of Catalysis, Siberian Branch of the Russian Academy of Sciences, 630090 Novosibirsk, Russian Federation*

DOI: 10.1016/j.mencom.2023.10.024

The effective surface concentration of Pd_1 sites composed of individual palladium atoms isolated from each other by Ag atoms in the Pd_1Ag_{10}/Al_2O_3 single-atom alloy (SAA) catalyst can be significantly enhanced by the adsorption-induced surface segregation upon a special pretreatment of the catalyst in a CO-containing atmosphere at 200 °C. The catalyst activity towards acetylene hydrogenation gets tripled without sacrificing selectivity for ethylene. The segregated surface of the catalyst is thus preserved under target reaction conditions.

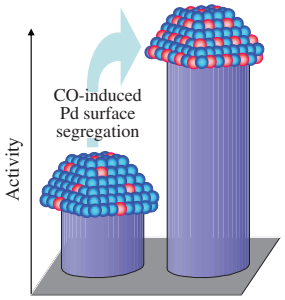

Keywords: single-atom alloy catalyst, adsorption-induced segregation, CO adsorption, selective acetylene hydrogenation, Pd, DRIFTS, XPS.

The article is dedicated to the 70th anniversary of Academician Mikhail P. Egorov.

Selective hydrogenation over supported bimetallic catalysts is widely used in laboratory and industry practice.[1–6] Thus, the selective acetylene-to-ethylene hydrogenation, also referred to as semi-hydrogenation of acetylene, is a highly industrially relevant process, especially for the large-scale polyethylene production.[7–9] Ethylene feedstock from naphtha cracking is contaminated with traces of acetylene, which have to be converted into ethylene to prevent the poisoning of polymerization catalysts and improve the net efficacy of the process. The Pd–Ag catalysts are most promising for this purpose.[10–13] The alloying of palladium with silver prevents the formation of palladium hydrides, which catalyze undesired total hydrogenation to ethane.[14] Furthermore, various Pd–Ag configurations can emerge at the surface of alloyed catalysts;[15–16] thus, an assortment of surface engineering tools have been elaborated[17,18] to preferentially construct a specific type of active sites within the single-atom alloy (SAA) paradigm.[4,19–22] Low-Pd dilute alloys frequently demonstrated an impressively high selectivity at the costs of only moderate activity. Recently, it was reported that adsorbate-induced segregation can be applied to overcome the problem of low activity,[23–25] but the issue remains insufficiently explored for the case of SAA catalysts.

Here, we demonstrate that the activity of a Pd_1Ag_{10}/Al_2O_3 single-atom alloy catalyst towards the selective hydrogenation of acetylene can be intentionally increased by adsorbate-induced segregation enabled by a simple pretreatment of the catalyst in CO.

To get insight into changes in the chemical state and catalyst surface structure driven by the CO-induced segregation, we used HRTEM, DRIFT spectroscopy of adsorbed CO, and XPS as most appropriate surface-sensitive techniques. An HRTEM micrograph of the freshly reduced Pd_1Ag_{10}/Al_2O_3 catalyst demonstrates nearly spherical bimetallic nanoparticles with sizes of 2–4 mm and a number-weighted mean diameter of 2.8 nm [Figure 1(*a*)]. HRTEM revealed no essential changes due to adsorbate induced segregation [Figure 1(*a*),(*b*)]. Indeed, the number-weighted mean size of PdAg particles after the CO treatment was about 2.9 nm, which indicates that the metal nanoparticles were not agglomerated.

Figure 2 shows the DRIFT spectra of the $PdAg_{10}/Al_2O_3$ catalyst before (reduced *in situ*) and after the CO-induced segregation.

The vibrational spectrum of the freshly reduced sample exhibited only one symmetrical band with a maximum at 2045 cm^{-1} corresponding to linearly bonded CO on palladium atoms. The significant bathochromic shift from ~2090–2085 cm^{-1} characteristic for monometallic palladium supported on Al_2O_3[26]

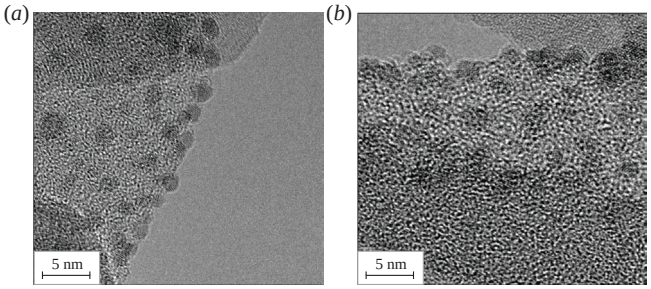

Figure 1 HRTEM micrographs of (*a*) the freshly reduced Pd_1Ag_{10}/Al_2O_3 catalyst and (*b*) the catalyst after CO-induced segregation at 200 °C.

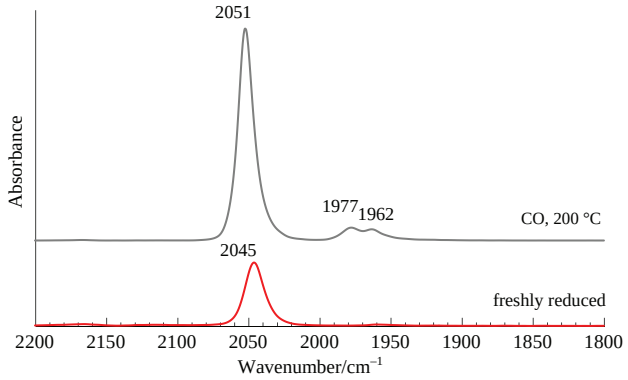

Figure 2 DRIFT spectra of CO adsorbed on a Pd_1Ag_{10}/Al_2O_3 sample (red) in a freshly reduced state and (grey) after CO-induced segregation at 200 °C.

towards 2045 cm^{-1} can be ascribed to weakened lateral interactions between adsorbed CO species on the Pd–Ag surface. Furthermore, a smaller wavenumber of linear CO is attributable to a modification of palladium electronic states due to the formation of PdAg alloy nanoparticles.

Note that no bands attributable to CO adsorbed on Ag atoms were observed in the spectra. According to published data,[27,28] CO bonding on the Ag surface can be detected only at ~ 90 K because of a low adsorption energy.

The absence of other bands in a range of 2000–1800 cm^{-1} indicates the complete disappearance of multiatomic palladium ensembles and the formation of a uniform SAA surface structure with isolated Pd_1 sites.

After the CO treatment at 200 °C, the peak intensity of linear CO increased by a factor of 3.4, and the peak shifted towards higher frequencies by 6 cm^{-1} (from 2045 to 2051 cm^{-1}). These changes suggest an increased number of Pd atoms available for the linear mode of CO adsorption after the CO-induced Pd surface segregation. Two minor bands appeared in the spectra at 1977 and 1962 cm^{-1} after the CO treatment. These bands can be ascribed to bridged CO species adsorbed on two adjacent palladium atoms. The presence of bridge-bonded CO indicated the appearance of a minor amount of palladium dimers (Pd_2 sites) on the catalyst surface.

The fraction of these Pd_2 sites (F_{Pd2}) on the catalyst surface was roughly estimated from the balance of linear and bridged CO band intensities according to the formula:

$$F_{Pd2} = I_{bridge}/(I_{linear} + I_{bridge}),$$

where I_{linear} and I_{bridge} are the integral intensities of linear CO and bridged CO peaks, respectively. The apparent value of F_{Pd2} is approximately 0.075. Note that the extinction coefficient for the bridged CO adsorption was higher by a factor of 20–25 than that for the linear adsorption mode.[29] Therefore, the net contribution of Pd_2 sites was negligible (F_{Pd2} < 0.3% of the total amount of Pd surface sites).

The effect exerted by the CO treatment at 200 °C on the $PdAg_{10}/Al_2O_3$ surface structure was also probed by XPS with a detailed comparative analysis of the spectra successively measured for a sample freshly reduced in H_2 at 500 °C and treated in CO at 200 °C (Figure 3). For the freshly reduced Pd_1Ag_{10}/Al_2O_3 catalyst, the binding energies of Pd $3d_{5/2}$ (334.2 eV) and Ag $3d_{5/2}$ (367.4 eV) core levels were shifted towards lower values with respect to the characteristic signals of metallic palladium and silver typical of alloyed PdAg nanoparticles.[26,30,31] The CO-treatment at 200 °C caused a positive shift of binding energies to 334.8 and 367.9 eV for Pd $3d_{5/2}$ and Ag $3d_{5/2}$, respectively; that is, they get close to the values typical of metallic Pd and Ag. According to published data, this behavior indicates changes in the composition and surface structure of bimetallic particles under the action of CO.[26,30–33]

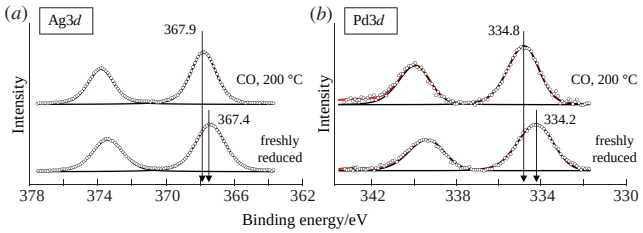

Figure 3 (*a*) Ag 3*d* and (*b*) Pd 3*d* spectra of the $PdAg_{10}/Al_2O_3$ catalyst in a freshly reduced state and after CO-induced segregation at 200 °C.

The surface atomic ratio Pd : Ag in the initial $PdAg_{10}/Al_2O_3$ catalyst was ~ 0.08, which is ~20% lower than the stoichiometric value due to an enrichment of the PdAg alloy surface with Ag atoms under ultra-high vacuum (UHV) conditions.[34–38] This Ag surface segregation was caused by a lower surface energy of Ag as compared to that of Pd.[13,14] It is well known that the surface energies of Pd and Ag differ by 25 kJ mol^{-1}, which is higher than the heat of the formation of a PdAg solid solution by a factor of 5.[35,39–41] As a result, the alloy surface was spontaneously enriched with the element possessing a lower surface energy. The CO treatment at 200 °C increased the Pd : Ag atomic ratio to 0.1, which corresponds to the nominal stoichiometry of Pd_1Ag_{10} bimetallic nanoparticles. This result clearly shows that the CO-induced segregation promoted an enrichment of PdAg nanoparticle surface with Pd atoms. Note that these data are consistent with the DRIFTS CO results.

The C 1*s* spectra (Figure S1) demonstrated that only traces of adventitious carbon (284.6 eV) were present on the surface, which is typical for XPS of supported catalysts. No additional carbon states appeared in C 1*s* after the treatment of catalysts in CO. This fact suggests the efficient desorption of CO from the surface of PdAg nanoparticles under UHV conditions when all CO was pumped out.

The effect of CO-induced segregation on the catalytic performance of $PdAg_{10}/Al_2O_3$ was tested in the selective hydrogenation of acetylene (Figure 4).

It is obvious that the CO treatment at 200 °C significantly increased the catalyst activity compared to that of the freshly reduced catalyst. Thus, the acetylene conversion at 70 °C increased from 17 to 60% after the CO-induced surface segregation, and the temperature of full C_2H_2 conversion decreased from 115 to 90 °C. The activity was improved in accordance with the characterization data indicating that the CO-induced segregation significantly increased the surface concentration of active Pd_1 sites, as jointly revealed by both DRIFTS CO and XPS experiments.

Remarkably, the excellent selectivity of the SAA catalyst for ethylene was not deteriorated by the CO treatment, although the activity increased by a factor of 3. This can be explained taking into account the DRIFTS CO results clearly showing that the efficient isolation of Pd_1 sites by Ag atoms was not violated by the CO-induced Pd surface segregation since the emergence

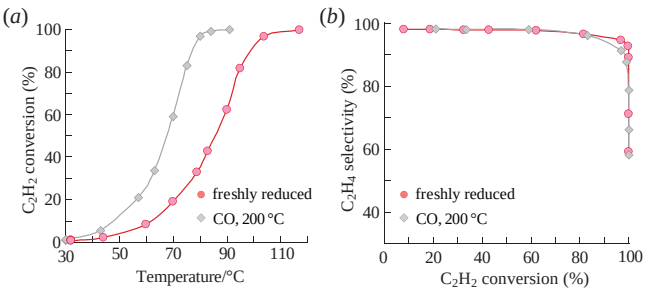

Figure 4 Effect of CO-induced segregation on the performance of the Pd_1Ag_{10}/Al_2O_3 catalyst in acetylene hydrogenation: (*a*) acetylene conversion as a function of reaction temperature and (*b*) selectivity for ethylene as a function of acetylene conversion.

of multinuclear Pd_n ($n > 2$) surface ensembles remained at a negligible level (see above).

Note that the improvement of catalyst activity was retained in the course of five consecutive catalytic measurements; that is, the positive effect of adsorbate-induced segregation was sufficiently stable.

Thus, the characterization data and the results of catalytic tests allowed us to conclude that the CO-induced surface segregation of Pd is a very facile and efficient means to increase the number of Pd_1 active sites on the surface of PdAg nanoparticles and improve the catalytic activity of the Pd_1Ag_{10}/Al_2O_3 SAA catalyst by a factor of more than 3 without a noticeable decrease in the selectivity for ethylene.

This work was supported by the Russian Science Foundation (grant no. 19-13-00285-P).

Online Supplementary Materials

Supplementary data associated with this article can be found in the online version at doi: 10.1016/j.mencom.2023.10.024.

References

1 B. S. Bal'zhinimaev, *Russ. Chem. Rev*., 2020, **89**, 1184.
2 Y. Ren, Y. Yang and M. Wei, *ACS Catal*., 2023, **13**, 8902.
3 K. N. Patil, P. Manikanta, P. M. Srinivasappa, A. H. Jadhav and B. M. Nagaraja, *J. Environ. Chem. Eng.*, 2023, **11**, 109168.
4 I. S. Mashkovsky, P. V. Markov, A. V. Rassolov, E. D. Patil and A. Yu. Stakheev, *Russ. Chem. Rev.*, 2023, **92**, RCR5087.
5 E. V. Shuvalova and O. A. Kirichenko, *Mendeleev Commun*., 2021, **31**, 875.
6 A. A. Shesterkina, A. A. Strekalova, E. V. Shuvalova, G. I. Kapustin, O. P. Tkachenko and L. M. Kustov, *Mendeleev Commun*., 2022, **32**, 672.
7 T. D. Shittu and O. B. Ayodele, *Front. Chem. Sci. Eng*., 2022, **16**, 1031.
8 Z. Wang, Q. Luo, S. Mao, C. Wang, J. Xiong, Z. Chen and Y. Wang, *Nano Res*., 2022, **15**, 10044.
9 L. Zhang, M. Zhou, A. Wang and T. Zhang, *Chem. Rev*., 2019, **120**, 683.
10 G. X. Pei, X. Y. Liu, A. Wang, A. F. Lee, M. A. Isaacs, L. Li, X. Pan, X. Yang, X. Wang, Z. Tai, K. Wilson and T. Zhang, *ACS Catal*., 2015, **5**, 3717.
11 M. R. Ball, K. R. Rivera-Dones, E. B. Gilcher, S. F. Ausman, C. W. Hullfish, E. A. Lebrón and J. A. Dumesic, *ACS Catal*., 2020, **10**, 8567.
12 J. Wang, H. Xu, C. Che, J. Zhu and D. Cheng, *ACS Catal*., 2022, **13**, 433.
13 K. S. Kley, J. De Bellis and F. Schüth, *Catal. Sci. Technol*., 2023, **13**, 119.
14 T. Mitsudome, T. Urayama, K. Yamazaki, Y. Maehara, J. Yamasaki, K. Gohara, Z. Maeno, T. Mizugaki, K. Jitsukawa and K. Kaneda, *ACS Catal*., 2016, **6**, 666.
15 X.-T. Li, L. Chen, C. Shang and Z.-P. Liu, *J. Am. Chem. Soc*., 2021, **143**, 6281.
16 N. S. Smirnova, G. N. Baeva, P. V. Markov, I. S. Mashkovsky, A. V. Bukhtiyarov, Ya. V. Zubavichus and A. Yu. Stakheev, *Mendeleev Commun.*, 2022, **32**, 807.
17 L. Mohrhusen, T. Egle, J. D. Lee, C. M. Friend and R. J. Madix, *J. Phys. Chem. C*, 2022, **126**, 20332.
18 I. A. Chetyrin, A. V. Bukhtiyarov, I. P. Prosvirin and V. I. Bukhtiyarov, *Mendeleev Commun.*, 2021, **31**, 635.
19 W. Guo, Z. Wang, X. Wang and Y. Wu, *Adv. Mater*., 2021, **33**, 2004287.
20 R. T. Hannagan, G. Giannakakis, M. Flytzani-Stephanopoulos and E. C. H. Sykes, *Chem. Rev*., 2020, **120**, 12044.
21 X. Liang, N. Fu, S. Yao, Z. Li and Y. Li, *J. Am. Chem. Soc*., 2022, **144**, 18155.
22 B. Singh, V. Sharma, R. P. Gaikwad, P. Fornasiero, R. Zbořil and M. B. Gawande, *Small*, 2021, **17**, 2006473.
23 A. Yu. Stakheev, N. S. Smirnova, P. V. Markov, G. N. Baeva, G. O. Bragina, A. V. Rassolov and I. S. Mashkovsky, *Kinet. Catal*., 2018, **59**, 610 (*Kinet. Katal*., 2018, **59**, 601).
24 M. A. van Spronsen, K. Daunmu, C. R. O'Connor, T. Egle, H. Kersell, J. Oliver-Meseguer, M. B. Salmeron, R. J. Madix, P. Sautet and C. M. Friend, *J. Phys. Chem. C*, 2019, **123**, 8312.
25 Z.-J. Wang, J. Chen, Y. Huang and Z.-X. Chen, *Mater. Today Commun*., 2021, **28**, 102475.
26 A. V. Rassolov, I. S. Mashkovsky, G. N. Baeva, G. O. Bragina, N. S. Smirnova, P. V. Markov, A. V. Bukhtiyarov, J. Wärnå, A. Yu. Stakheev and D. Yu. Murzin, *Nanomaterials*, 2021, **11**, 3286.
27 K. I. Hadjiivanov and G. N. Vayssilov, *Adv. Catal*., 2002, **47**, 307.
28 X.-D. Wang and R. G. Greenler, *Surf. Sci. Lett*., 1990, **226**, L51.
29 A. J. McCue and J. A. Anderson, *J. Catal*., 2015, **329**, 538.
30 D. V. Glyzdova, T. N. Afonasenko, E. V. Khramov, N. N. Leont'eva, I. P. Prosvirin, A. V. Bukhtiyarov and D. A. Shlyapin, *Appl. Catal., A*, 2020, **600**, 117627.
31 A. V. Bukhtiyarov, M. A. Panafidin, I. P. Prosvirin, I. S. Mashkovsky, P. V. Markov, A. V. Rassolov, N. S. Smirnova, G. N. Baeva, C. Rameshan, R. Rameshan, Ya. V. Zubavichus, V. I. Bukhtiyarov and A. Yu. Stakheev, *Appl. Surf. Sci*., 2022, **604**, 154497.
32 A. V. Bukhtiyarov, I. P. Prosvirin, A. A. Saraev, A. Y. Klyushin, A. Knop-Gericke and V. I. Bukhtiyarov, *Faraday Discuss*., 2018, **208**, 255.
33 D. V. Demidov, I. P. Prosvirin, A. M. Sorokin and V. I. Bukhtiyarov, *Catal. Sci. Technol*., 2011, **1**, 1432.
34 T. Marten, O. Hellman, A. V. Ruban, W. Olovsson, C. Kramer, J. P. Godowski, L. Bech, Z. Li, J. Onsgaard and I. A. Abrikosov, *Phys. Rev. B*, 2008, **77**, 125406.
35 P. T. Wouda, M. Schmid, B. E. Nieuwenhuys and P. Varga, *Surf. Sci*., 1998, **417**, 292.
36 O. M. Løvvik, *Surf. Sci*., 2005, **583**, 100.
37 J. R. Kitchin, K. Reuter and M. Scheffler, *Phys. Rev. B*, 2008, **77**, 075437.
38 B. C. Khanra and M. Menon, *Physica B: Condensed Matter*, 2000, **291**, 368.
39 H. L. Skriver and N. M. Rosengaard, *Phys. Rev. B*, 1992, **46**, 7157.
40 M. Methfessel, D. Hennig and M. Scheffler, *Phys. Rev. B*, 1992, **46**, 4816.
41 J. P. Chan and R. Hultgren, *J. Chem. Thermodyn*., 1969, **1**, 45.

Received: 9th August 2023; Com. 23/7223